Human Reproduction, Vol.31, No.4 pp. 734–749, 2016
Advanced Access publication on February 22, 2016 doi:10.1093/humrep/dew018

human reproduction

ORIGINAL ARTICLE *Gynaecology*

Corroborating evidence for platelet-induced epithelial-mesenchymal transition and fibroblast-to-myofibroblast transdifferentiation in the development of adenomyosis†

Xishi Liu[1,2,‡], Minhong Shen[1,‡], Qiuming Qi[1], Hongqi Zhang[3], and Sun-Wei Guo[1,2,*]

[1]Shanghai OB/GYN Hospital, Fudan University, Shanghai 200011, China [2]Shanghai Key Laboratory of Female Reproductive Endocrine-Related Diseases, Fudan University, Shanghai, China [3]Department of Anatomy, Histology and Embryology, Shanghai Medical Collage, Fudan University, Shanghai, China

*Correspondence address. Shanghai Obstetrics and Gynecology Hospital, Fudan University, 419 Fangxie Road, Shanghai 200011, China. Fax: +86-21-6345-5090; E-mail: hoxa10@outlook.com

Submitted on July 3, 2015; resubmitted on January 16, 2016; accepted on January 21, 2016

STUDY QUESTION: Do platelets play any role in the development of adenomyosis?

SUMMARY ANSWER: As in endometriosis, adenomyotic lesions show significantly increased platelet aggregation, increased expression of transforming growth factor (TGF)-β1, phosphorylated Smad3, markers of epithelial-mesenchymal transition (EMT) and fibroblast-to-myofibroblast transdifferentiation (FMT), and smooth muscle metaplasia (SMM), in conjunction with increased fibrosis as compared with normal endometrium.

WHAT IS KNOWN ALREADY: Both EMT and FMT are known to play vital roles in fibrogenesis in general and in endometriosis in particular. EMT has been implicated in the development of adenomyosis. SMM is universally seen in endometriosis and also in adenomyosis, and is correlated positively with the extent of fibrosis. However, there has been no published study on the role of platelets in fibrogenesis in adenomyosis, even though adenomyotic lesions undergo repeated cycles of tissue injury and repair, which suggests the involvement of platelets and their possible roles in fibrogenesis.

STUDY DESIGN, SIZE, DURATION: Cross-sectional studies of ectopic endometrial and control endometrial tissue samples from three sets of women with and without adenomyosis ($n = 34$ and 20, 12 and 10, and 8 and 8, respectively) were carried out from 2014 to 2015.

PARTICIPANTS/MATERIALS, SETTING, METHODS: Immunohistochemistry analysis of ectopic endometrial tissues from women with ($n = 34$) and without ($n = 20$) adenomyosis with respect to biomarkers of EMT, FMT and highly differentiated smooth muscle cells as well as TGF-β1, phosphorylated Smad3, markers of proliferation, angiogenesis and extracellular matrix (ECM) deposits. Masson trichrome staining, Van Gieson staining and Pico-Sirius staining were performed to evaluate and quantify the extent of fibrosis in lesions. Progesterone receptor isoform B (PR-B) staining also was performed. In addition, CD42b-positive platelets in ectopic ($n = 12$) and control ($n = 10$) endometrium were counted by confocal microscopy and compared. The protein expression levels of TGF-β1 and phosphorylated Smad3 in both ectopic ($n = 8$) and control ($n = 8$) endometrium were measured by western blot analysis. Immunofluorescent staining of both platelets and hepatocyte growth factor (HGF) was also performed for adenomyotic tissue samples ($n = 10$).

MAIN RESULTS AND THE ROLE OF CHANCE: Adenomyotic lesions had a significantly higher extent of platelet aggregation and increased staining for TGF-β1 and phosphorylated Smad3 (both *P*-values <0.001 versus control). In addition, E-cadherin staining was decreased while vimentin staining in adenomyotic epithelial cells was increased, along with increased staining of proliferating cell nuclear antigen, vascular endothelial growth factor and CD31 (all *P*-values <0.001), markers of proliferation and angiogenesis. Staining for α-SMA, a marker for

†This paper has been presented orally at the First Congress of the Society of Endometriosis and Uterine Disorders (SEUD) held in Paris on 9 May 2015.

‡ These two authors contributed equally to this work.

© The Author 2016. Published by Oxford University Press on behalf of the European Society of Human Reproduction and Embryology. All rights reserved.
For Permissions, please email: journals.permissions@oup.com

Downloaded from https://academic.oup.com/humrep/article/31/4/734/2380144 by guest on 21 August 2022

myofibroblast, desmin, smooth muscle myosin heavy chain and oxytocin receptor was significantly increased in adenomyotic lesions versus control, concomitant with increased staining of collagen I and lysyl oxidase (all *P*-values <0.001). Histochemistry analysis indicates that the extent of fibrosis is high in adenomyotic lesions ($P < 0.001$), and the extent appeared to correlate negatively with the microvessel density ($P < 0.05$). PR-B staining was significantly decreased in adenomyotic lesion as compared with control endometrium ($P < 0.001$). Platelets and HGF were co-localized mostly in the stromal component of adenomyotic lesions, near the glandular epithelium.

LIMITATIONS, REASONS FOR CAUTION: The results are limited by the cross-sectional nature of the study and the use of histochemistry and immunohistochemistry analyses only, but nonetheless is a validation of our previous finding in mouse experiments.

WIDER IMPLICATIONS OF THE FINDINGS: The data presented are consistent with the notion that platelet-induced activation of the TGF-β/Smad signaling pathway may be a driving force in EMT, FMT and SMM in the development of adenomyosis, leading to fibrosis. This study provides the first piece of evidence that adenomyotic lesions are wounds that undergo repeated injury and healing, and, as such, platelets play critical roles in the development of adenomyosis by promoting proliferation, angiogenesis, increasing ECM deposits, and SMM, resulting in fibrosis. Platelets may also be involved in uterine hyperactivity and myometrial hyperinnervation. Our results provide one explanation as to why adenomyosis is a challenge for medical treatment, and shed new light onto the pathophysiology of adenomyosis.

STUDY FUNDING/COMPETING INTERESTS: Support for data collection and analysis was provided by grants from the National Science Foundation of China. None of the authors has anything to disclose.

Key words: adenomyosis / epithelial-mesenchymal transition / fibroblast-to-myofibroblast transdifferentiation / fibrosis / platelet / smooth muscle metaplasia / transforming growth factor-β1

Introduction

Adenomyosis is a common gynecologic disorder with poorly understood pathogenesis and pathophysiology (Bergeron *et al.*, 2006; Benagiano *et al.*, 2012). Besides a soft and diffusely enlarged uterus, its symptoms also include dysmenorrhea, heavy menstrual bleeding, and subfertility (Farquhar and Brosens, 2006). Treatment of adenomyosis is challenging, with hysterectomy being the treatment of choice (Bergeron *et al.*, 2006). Although the disease is hormone-sensitive (Kitawaki, 2006), progestogenic agents are not very effective, and the efficacy of GnRH agonists is restricted by their short duration (Bergeron *et al.*, 2006). In addition, the symptoms often recur after discontinuation of GnRH agonists therapy (Grow and Filer, 1991).

Emerging evidence suggests that epithelial-mesenchymal transition (EMT) may play a role in the development of adenomyosis, resulting in an increased invasive propensity of adenomyotic epithelial cells (Chen *et al.*, 2010). Oh *et al.* reported elevated levels of nuclear β-catenin in adenomyosis and found that stabilized β-catenin expression in mouse resulted in changed expression of EMT markers, such as E-cadherin, SNAIL and ZEB1, concomitant with increased incidence of adenomyosis (Oh *et al.*, 2013). Khan *et al.* reported increased hepatocyte growth factor (HGF) levels in the endometrial-myometrial junction in adenomyosis, HGF-mediated EMT along with increased migratory ability in HGF-treated endometrial epithelial cells, and also signs of EMT in Ishikawa cells treated with HGF (Khan *et al.*, 2015).

While a role for EMT in the development of adenomyosis is intuitively plausible, it is unclear as to whether adenomyotic lesions and/or their micro-environment have *all* the necessary molecular machinery that promotes EMT. For example, where is the source of HGF? What induces β-catenin overexpression in adenomyosis? In addition, while EMT is known to occur in tissue repair (Thiery *et al.*, 2009) and often leads to fibrosis (Nawshad *et al.*, 2004), it is unclear whether fibrosis also is present in adenomyosis as in endometriosis (Matsuzaki and Darcha, 2013). However, the presence of smooth muscle metaplasia (SMM) in adenomyosis (Mechsner *et al.*, 2010) and its documented correlation with the extent of fibrosis in endometriosis (Itoga *et al.*, 2003) suggest that fibrosis should be present in adenomyosis.

As in endometriosis and eutopic endometrium, the ectopic endometrium in adenomyosis also experiences cyclic bleeding—a cardinal sign of tissue injury. As such, it undergoes cyclic or repeated tissue injury and repair, a process very similar to what happened in the development of endometriosis (Ding *et al.*, 2015). Since it is well known that repeated tissue injury causes fibrosis (Wynn, 2007), the same process apparently leads to an increased extent of fibrosis in ovarian endometriomas (Guo *et al.*, 2015) and may also lead to fibrosis in adenomyosis. Indeed, increased collagen content in adenomyosis has been documented, although not in the mainstream journals (Fujita, 1985, Ikegami and Kato, 1992).

We have recently found that activated platelets induce activation of the transforming growth factor (TGF)-β1/Smad3 signaling pathway in endometriotic epithelial and stromal cells, resulting in EMT, fibroblast-to-myofibroblast transdifferentiation (FMT), increased cellular migratory and invasive propensity, and increased cell contractility and collagen production, leading to SMM and ultimately to fibrosis (Zhang *et al.*, submitted for publication). Capitalizing on these findings and employing a mouse model of adenomyosis (Parrott *et al.*, 2001), we conducted a mouse study that examined (through immunohistochemistry (IHC)) platelet aggregation, EMT, FMT, TGF-β1, phosphorylated Smad3 (p-Smad3), and collagen I, and the extent of fibrosis through serial observation. Consistent with the finding in endometriosis, we found that staining of markers of EMT and FMT became progressively more pronounced as adenomyosis progressed along, with a gradual but progressive increase in expression of TGF-β1 and phosphorylated Smad3, leading to increased fibrotic tissue content in adenomyotic lesions (Shen *et al.*, 2016).

This study sought to confirm these findings in human adenomyosis. We hypothesized that both EMT and FMT, driven by platelet-derived TGF-β1 and platelet-induced TGF-β1/Smad3 activation, occur in the development of adenomyosis, leading to SMM and eventually to increased fibrotic tissue content in lesions. To test this hypothesis, we performed an IHC analysis of TGF-β1 and p-Smad3 expression and of

Downloaded from https://academic.oup.com/humrep/article/31/4/734/2380144 by guest on 21 August 2022

EMT and FMT markers, along with markers of proliferation, angiogenesis, extracellular matrix (ECM) components as well as markers of fully differentiated smooth muscle cells (SMCs) such as desmin, smooth muscle myosin heavy chain (SM-MHC), and oxytocin receptor (OTR) in ectopic endometrial tissue samples from women with adenomyosis and control endometrial tissue samples. In addition, we evaluated the extent of platelet aggregation in both types of tissue samples. Moreover, we performed a histochemistry analysis of the extent of fibrosis, and evaluated the protein expression of TGF-β1 and p-Smad3. We found that our results are completely consistent with the hypothesis. Finally, we carried out an immunofluorescent staining of both platelets and HGF in adenomyotic lesions to see whether platelets may also be responsible for the reported HGF-induced EMT in adenomyosis. Since the serial observation of human adenomyosis as it develops is out of the question, naturally only the cross-sectional data are presented. Nonetheless, our human data appear to dovetail all key events of a chain of changes as stipulated the hypothesis, providing corroborative evidence for the hypothesis.

Materials and Methods

Patients and tissue samples

Thirty-four women with adenomyosis (excluding endometriosis) seen at Shanghai OB/GYN Hospital, Fudan University, from 2013 to 2014, were recruited for this study. Their diagnoses were made by transvaginal ultrasound before surgery and histologically confirmed post-operatively. After obtaining written informed consent their ectopic endometrial tissue samples were collected during hysterectomy and immediately fixed in 10% buffered formalin and then processed for paraffin embedding. For controls, we also collected, after informed consent, endometrial tissue samples through curettage from 20 women with teratoma ($n = 1$, 5%), cervical intraepithelial neoplasia (CIN)-III ($n = 14$, 70%), stage Ia1 cervical cancer ($n = 3$, 15%), and cervical carcinoma *in situ* ($n = 2$, 10%), but without any clinical indication or history of adenomyosis or endometriosis. The selection of the controls was based solely on menstrual phase besides disease status.

Except for 6 women in the adenomyosis group, who had irregular cycles, all other women in both study and control groups had regular cycles. All women in both study and control groups were premenopausal and had no hormone therapy or intrauterine device use for ≥6 months prior to tissue collection. The menstrual phase was determined by histological endometrial dating. The amount of menses during menstruation was grouped into three classes: light, moderate, and heavy, depending on whether they changed their sanitary pads <3, between 3 and 6, or >6 times a day, respectively (Hernandez Guerrero *et al.*, 2006).

For each patient with adenomyosis, the following information was collected through reading medical charts and interviewing: age at surgery, uterus size (calculated as $\pi D_1 D_2 D_3/6$, where D_1 = the distance from fundus to the internal os of the cervix, D_2 = transverse diameter at the level of the cornua, and D_3 = anteroposterior diameter at the level of cornua), complaint of dysmenorrhea, duration of dysmenorrhea, amount of menses (light, moderate, or heavy), and parity. The severity of dysmenorrhea was quantified using a 10-cm visual analog scale, assessed before operation.

For immunofluorescent staining analysis of platelet aggregation, additional tissue samples of ectopic endometrium from 12 women with adenomyosis and control endometrial tissue samples from 10 age- and menstrual phase-matched women who underwent surgery for benign gynecologic disorders but free of endometriosis and adenomyosis were collected. The mean age of controls and adenomyosis patients were 42.3 (±4.4) and 44.3 (±4.6) years, respectively ($P = 0.49$, Wilcoxon test). Two tissue samples (20.0%) in the control group and 2 in the adenomyosis group (16.7%) were in the proliferative phase ($P = 1.0$, Fisher's exact test). The diagnoses of the 12 women with adenomyosis were made also by transvaginal ultrasound before surgery and were histologically confirmed post-operatively.

For immunofluorescent staining analysis of HGF and platelets, additional adenomyotic samples from 12 women with adenomyosis and control endometrial tissue samples from 10 age- and menstrual phase-matched women without adenomyosis or endometriosis were collected (CIN, $n = 5$, stage Ia1 cervical cancer, $n = 3$, and cervical carcinoma *in situ*, $n = 2$). The mean age of controls and adenomyosis patients was 42.3 (±4.4) and 44.3 (±4.6) years, respectively ($P = 0.49$). Two controls (20.0%) and 2 in the adenomyosis group (16.7%) were in the proliferative phase ($P = 1.0$, Fisher's exact test). The diagnosis of the 12 women with adenomyosis was made by transvaginal ultrasound before surgery and histologically confirmed post-operatively. For controls, endometrial tissue samples were collected through curettage. The selection of the controls was also based solely on age and menstrual phase besides disease status.

For western blot analysis, adenomyotic tissue samples from 8 women with adenomyosis and control endometrial tissue samples from 8 women who underwent surgery for benign gynecologic disorders without adenomyosis or endometriosis were collected. The mean age of controls was younger than that of adenomyosis patients (37.1 ± 7.0 versus 44.6 ± 3.9 years, respectively, $P = 0.03$). The diagnosis of adenomyosis was made in the same manner as described above. All tissue samples were collected during the operation. The selection of the controls was based solely on menstrual phase besides disease status.

This study was approved by the institutional Ethics Review Committee of Shanghai OB/GYN Hospital.

IHC

Serial 4-μm sections were obtained from each paraffin-embedded tissue block, with the first resultant slide being stained for H&E to confirm pathologic diagnosis and the subsequent slides used for IHC. Routine deparaffinization and rehydration procedures were performed as reported previously (Ding *et al.*, 2015).

The antibodies used as primary antibodies for immunohistochemistry analysis are listed in Supplementary Table SI. For antigen retrieval, the slides were heated at 98°C in an EDTA buffer (pH 9.0) for a total of 20 min (proliferating cell nuclear antigen (PCNA), phosphorylated Smad3 (p-Smad3), lysyl oxidase (LOX), and progesterone receptor isoform B (PR-B)) or in a citrate buffer (pH 6.0) for a total of 30 min (TGF-β1, E-cadherin, vimentin, α-smooth muscle actin (α-SMA), vascular endothelial growth factor (VEGF), CD31, CD41, collagen I, desmin, smooth muscle myosin heavy chain (SM-MHC), and oxytocin receptor (OTR)), and cooled at room temperature. Sections were then incubated overnight with the primary antibody at 4°C. After slides were rinsed, the biotinylated secondary antibody, Supervision TM Universal (Anti-Mouse/Rabbit) Detection Reagent (HRP) (GK500705, Shanghai GeneTech Company, Shanghai, China), was used for incubation at room temperature for 30 min. The bound antibody complexes were stained for 3–5 min or as appropriate for microscopic examination with diaminobenzidine and then counterstained with hematoxylin and mounted.

Immunostaining results for CD41, PCNA, VEGF, TGF-β1, p-Smad3, E-cadherin, vimentin, α-SMA, collagen I, LOX, PR-B, desmin, SM-MHC, and OTR were evaluated using a semi-quantitative scoring system, as reported previously (Shen *et al.*, 2009). Briefly, images were obtained with a microscope (Olympus BX51, Olympus, Tokyo, Japan) fitted with a digital camera (Olympus DP70, Olympus), and the number and intensity of positive cells were counted by Image Pro-Plus 6.0 (Media Cybernetics, Inc., Bethesda, MD, USA) blind to which group the slide belonged to. A series of 5 images randomly selected from several sections per tissue sample were taken for

Downloaded from https://academic.oup.com/humrep/article/31/4/734/2380144 by guest on 21 August 2022

each immunostaining parameter to obtain a mean value. The CD31 labeled microvessel density (MVD) was counted under 400× high-power (Hp) microscopy, as reported previously (Shen *et al.*, 2009).

The epithelial and stromal components were jointly evaluated for vimentin, TGF-β1, p-Smad3, α-SMA, collagen I, VEGF, PCNA and LOX, which were stained positive in both epithelial and stromal cells. However, only the epithelial component of TGF-β1, PCNA and VEGF staining was used for analysis because of their predominance in that component. E-cadherin and PR-B were stained positive only in epithelial cells, therefore only epithelial cells were evaluated. CD41 staining of platelets was seen primarily in the stromal component of adenomyotic lesions, and was evaluated only in the stroma. CD31 was stained positive exclusively in the epithelium of blood vessels, and as such MVD was calculated and averaged over five randomly selected areas of vessels (except large vessels) in adenomyotic lesions. Desmin, SM-MHC and OTR staining was positive not only in the smooth muscle tissues but also in the stroma, but only the stromal part was evaluated. To minimize potential bias, the person who evaluated the slides was blinded as to which group the slides belonged to.

Following vendors' protocols of the primary antibodies, mouse spleen tissues were used for the positive immunostaining of CD41 and vimentin, and human breast cancer tissues were used for the positive immunostaining of E-cadherin, p-Smad3, collagen I and PR-B, while mouse liver tissues were used for positive immunostaining of other markers. For the negative controls, human ectopic endometrium tissue samples were incubated with rabbit or mouse serum instead of primary antibodies. The representative examples of positive and negative staining results are shown in Supplementary Fig. S1.

Masson trichrome staining

Masson trichrome staining was used for the detection of collagen fibers in tissue samples. Tissue sections were deparaffinized in xylene and rehydrated in an increasing graded alcohol series, then were fixed in Bouin's solution at 37°C for 2 h. The Bouin's solution was made with 75 ml of saturated picric acid, 25 ml of 10% formalin solution (v/v), and 5 ml of acetic acid. Tissue sections were then stained using Masson's Trichrome Staining kit (Baso, Wuhan, China) following the manufacturer's instructions. The areas of the collagen fiber layer stained in blue relative to the entire portion of the ectopic implants were calculated by the Image Pro-Plus 6.0 (Media Cybernetics, Inc., Bethesda, MD, USA).

Van-Gieson staining

After heating at 60°C for 45 min, tissue sections were deparaffinized in xylene and rehydrated in a graded alcohol series. To stain nuclei, sections were dipped into Weigert iron hematoxylin for 10 min, rinsed with tap water, then dipped into 0.1% HCl- ethanol (v/v) for 10 s, and washed with tap water. The sections were then counterstained with Van Gieson solution (Goodbio, Wuhan, China) for 5 min before rinsing with tap water. The areas of the collagen fiber layer stained in red relative to the entire portion of the ectopic implants were calculated by the Image Pro-Plus 6.0 and used as the extent of fibrosis in the lesion.

Picro-Sirius red staining for collagen

Tissue sections were heated in an oven at 60°C for 45 min, and then deparaffinized in xylene and hydrated using increasing graded ethanol solutions.

Table I Characteristics of patients recruited with adenomyosis and controls.

Item	Controls ($n = 20$)	Adenomyosis ($n = 34$)	Statistical significance[a]
Age (year)	Mean = 38.5 (SD = 7.3) Median = 40.5 Range = 25–48	Mean = 44.6 (SD = 5.4) Median = 45.0 Range = 29–52	**
Menstrual phase			
Proliferative	10 (50.0%)	12 (35.3%)	NS
Secretory	10 (50.0%)	22 (64.7%)	
Parity			
0	5 (25.0%)	4 (11.8%)	NS
1	12 (60.0%)	22 (64.7%)	
≧2	3 (15.0%)	8 (23.5%)	
Visual analog scale on the severity of dysmenorrhea	Mean = 0.5 (SD = 1.3) Median = 0.0 Range = 0–5	Mean = 4.3 (SD = 2.9) Median = 5.0 Range = 0–8	***
Uterus size (cm^3)	Median = 70.4 Range = 31.5–113.9 Missing: $n = 1$	Median = 229.6 Range = 78.5–618.2	***
Co-occurrence of endometriosis			
No	20 (100.0%)	25 (73.5%)	*
Yes	0 (0.0%)	9 (26.5%)	
Co-occurrence of uterine fibroids			
No	19 (95.0%)	33 (97.1%)	NS
Yes	1 (5.0%)	1 (2.9%)	

[a]*$P < 0.05$; **$P < 0.01$; ***$P < 0.001$; NS: $P > 0.05$. Wilcoxon's rank test was used for age, visual analog scale and uterus size while for other data Fisher's exact test was used.

Downloaded from https://academic.oup.com/humrep/article/31/4/734/2380144 by guest on 21 August 2022

The tissue slides were placed in a Picro-Sirius red stain solution kit (Goodbio) for 20 min following the manufacturer's instructions, and rinsed with tap water for 1 min. Under the optical microscope, collagen fibers were stained in red while the epithelium, blood vessels and muscle appear yellowish. Under the dark zone of the microscope equipped with filters to provide circularly polarized illumination, the collagen fibers appeared bright while the interstitial space and non-collagen elements appeared darker. Collagen I fibrils appeared red and yellow, while collagen III fibrils appeared green.

Immunofluorescent staining and confocal microscopy

After antigen retrieval at 95°C in citrate buffer (pH 6) for a total of 30 min, serial 4 μm paraffin sections were cooled to room temperature and washed 3 times in phosphate-buffered saline (PBS). Five percent goat serum was used for blocking nonspecific binding. The slides were incubated overnight at 4°C with primary antibodies (listed in Supplementary Table SI), followed by washing in PBS thrice, and then incubated at 37°C with secondary antibodies (1: 500 AlexaFluor 647-conjugated goat anti-rabbit secondary Ab and 1: 500 AlexaFluor 488-conjugated goat anti-mouse secondary Ab; Cell Signaling Technology, Inc., Boston, MA, USA) for 1 h. After washing in PBS thrice, cell nuclei was counterstained with 4′,6-diamidino-2-phenylindole (DAPI) (Beyotime, Shanghai, China).

Fluorescent histologic slides were examined under a confocal laser scanning microscope (Leica TCS SP5 Confocal Microscope, Solms, Germany) at room temperature. Images were separately recorded with different objective lenses (40/1.3 NA oil and 100× objective), and then exported as a TIFF-format digital file. Image-Pro Plus (version 6.0.0.206, Media Cybernetics, Inc., Bethesda, MD, USA) was used to process the images (brightness and contrast), and to construct merged images for triple immunohistochemistry. For each slide, the number of CD42b labeled platelets was counted under a 400× Hp microscopy via Image-Pro Plus, and the operator was blinded to which group the slide belonged to. A cluster of or a single CD42b-positive platelet was counted as one.

Cell culture

The isolation and culture of adenomyosis-derived primary ectopic endometrial stromal cells (EESC) and normal endometrial stromal cells (NESC) derived from control endometrial tissues were carried out as reported previously (Ryan *et al.*, 1994). Briefly, adenomyotic tissues were minced into small pieces of about 1 mm^3. After the enzymatic digestion of minced tissues with 0.2% collagenase II (Sigma, St Louis, MO, USA) for 1.5 h at 37°C, they were separated by filtration through a 149 μm then a 37 μm (pore size) nylon mesh, removing the debris and epithelial and SMCs, respectively. Stromal cells remaining in the filtrate were collected by centrifugation, resuspended in Dulbecco's Modified Eagle's Medium (DMEM)/F12, and plated onto 10 cm dishes and allowed to adhere at 37°C for 30 min, after which non-adhering epithelial cells, myometrial SMCs, and blood cells were removed with PBS rinses. The cells were cultured in DMEM/F12 reconstituted with 10% charcoal-stripped fetal bovine serum and 1% antibiotics. The purity and homogeneity of the stromal cell preparation (≥98%) were verified by immunocytochemistry using an antibody against vimentin (Abcam), a specific marker of stromal cells, and an antibody against cytokeratin 7 (CK7) (Zhongshan Jinqiao, Beijing, China), a specific marker of epithelial cells. After 3–4 passages, the vimentin staining was positive, while CK7 staining was negative.

Western blot analysis

For total protein extraction, EESCs ($n = 8$) were scraped and extracted in a Radio-Immunoprecipitation Assay (RIPA) buffer (Fermentas, Burlington, CA, USA). Protein concentration was determined using the BCA protein quantitative analysis kit (P0010S, Beyotime). All proteins were mixed with sodium dodecyl sulfate polyacrylamide gel electrophoresis (SDS-PAGE) loading buffer (P0015, Beyotime) and heated for 8 min at 95°C for denaturation. Protein samples were loaded on a 10% SDS polyacrylamide gel, and electroblotted onto a polyvinyl difluoride (PVDF) membrane (Bio-Rad, Hercules, California, USA). The blots were blocked in 5% non-fat milk reconstituted in TBST (0.15 M NaCl, 0.05% Tween-20, 10 mM Tris–HCl [pH 8.0]) for 1 h at room temperature and subsequently incubated at 4°C overnight with the following primary antibodies: rabbit anti-human TGF-β1(1:1000), rabbit anti-human p-Smad3(1:1000), and rabbit anti-human GAPDH primary antibody (1:1000, CST, Danvers, MA, USA), where GAPDH was used as the loading control for total protein amount. After the membranes were incubated with

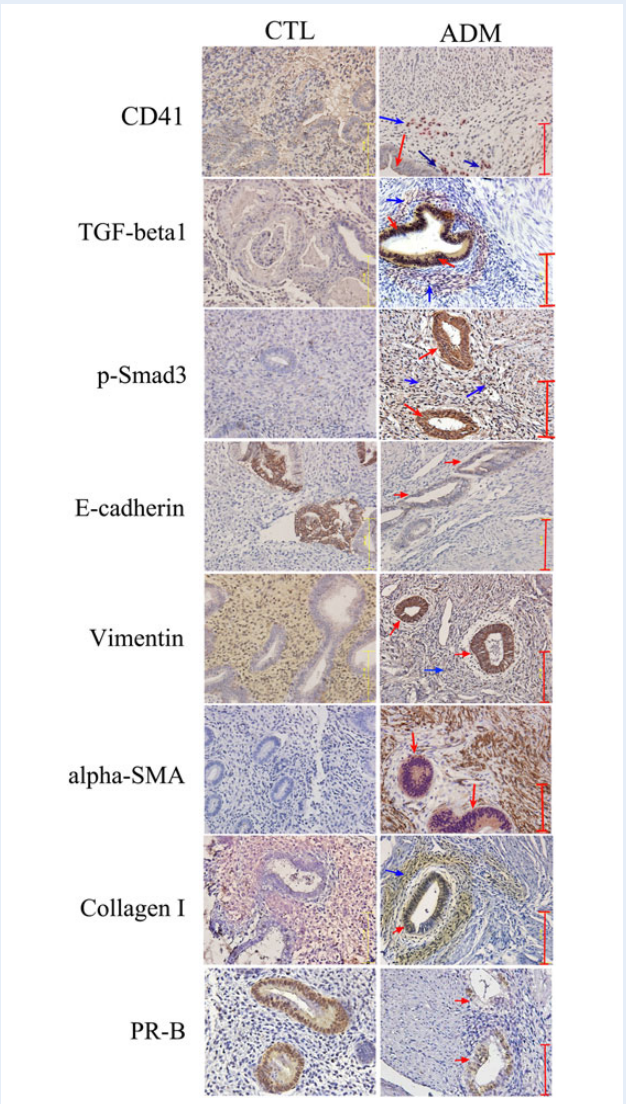

Figure 1 Representative results of indicated immunoreactivity staining in adenomyosis and control endometrium. TGF-β1: transforming growth factor-β1; p-Smad3: phosphorylated Smad3; α-SMA: α-smooth muscle actin; PR-B: progesterone receptor isoform B; CTL: control endometrium; ADM: ectopic endometrium from women with adenomyosis. The red arrows indicate epithelial cells, while the blue ones indicate stromal cells. Scale bar = 125 μm.

Downloaded from https://academic.oup.com/humrep/article/31/4/734/2380144 by guest on 21 August 2022

HRP-labeled secondary antibodies for 1 h at room temperature, the signal was detected using enhance chemiluminescence reagents (Pierce, Thermo Scientific, Rockford, IL, USA) on hyperfilms. The amount of protein expression was quantified by Quantity One software (Bio-Rad, Hercules, CA, USA).

Statistical analysis

For descriptive statistics, we used boxplot (Tukey, 1977) to graphically depict groups of immunoreactivity data. The comparison of distributions of continuous variables between or among two or more groups was made using the Wilcoxon test and Kruskal–Wallis test, respectively. Jonckheere–Terpstra trend test was used to test for trend of increasing immunostaining levels in women who complained of dysmenorrhea of varying severity. Pearson's or Spearman's rank correlation coefficient was used when evaluating correlations between two variables when both variables are continuous or when at least one variable is ordinal. The relationship between various clinical and pathological parameters was compared with chi-square tests.

To evaluate whether the source of tissue samples is associated with the differences in immunoreactivity, the number of aggregated platelets and the extent of fibrosis while controlling for other factors, such as menstrual phase and age, multiple linear regression analysis was used. Since no collagen fibers were detected in control endometrium, we assigned the Masson staining level as 0. Similarly, staining levels of desmin and others in control endometrium were recorded as 0.

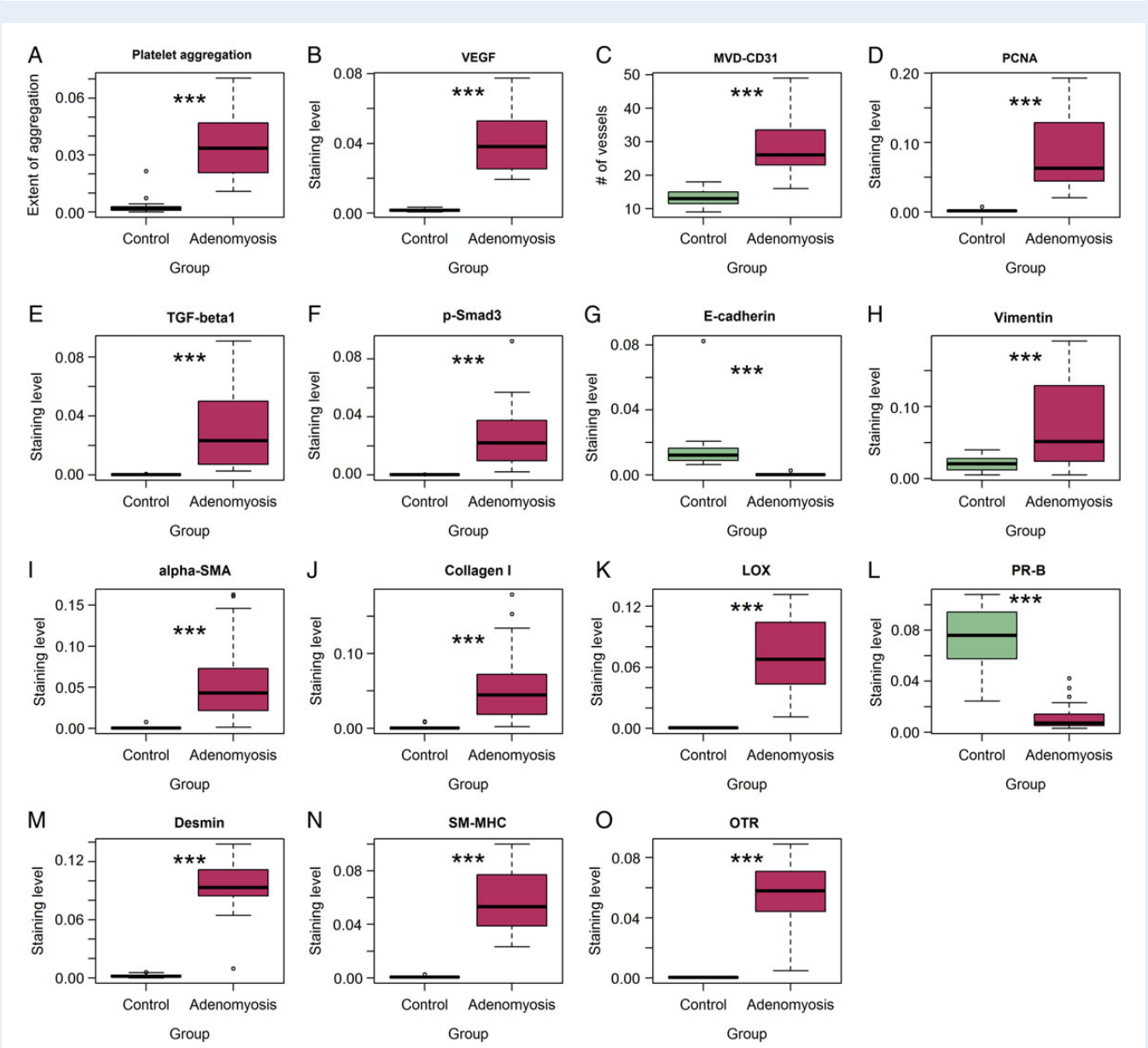

Figure 2 Boxplots of staining levels in adenomyotic lesions and control endometrium. (**A**) The extent of platelet aggregation (CD41); (**B**) VEGF; (**C**) microvessel density (CD31); (**D**) PCNA; (**E**) TGF-β1; (**F**) phosphorylated-Smad3; (**G**) E-cadherine; (**H**) Vimentin; (**I**) α-SMA; (**J**) Collagen I; (**K**) The extent of fibrosis; (**L**) PR-B; (**M**) Desmin; (**N**) SM-MHC; (**O**) Oxytocin receptor (OTR). ***$P < 0.001$. In all boxplots, the bottom and top of the box represent the lower and upper quartiles, respectively, the band near the middle of the box represents the median, and the ends of the whiskers represent the smallest and the largest non-outlier observations. The dots outside the box, if any, are outliers.

Downloaded from https://academic.oup.com/humrep/article/31/4/734/2380144 by guest on 21 August 2022

P-values of less than 0.05 were considered statistically significant. All computations were made with R 3.2.2 (Inhaka and Gentleman, 1996) (www.r-project.org).

Results

Clinicopathological data

Among the 34 patients with adenomyosis, only 1 (2.9%) had focal adenomyosis and the remaining 33 (97.1%) were of diffused type. The characteristics of the patients and the control subjects are shown in Table I. The controls were comparable with the cases in menstrual phase and parity but were significantly younger than patients with adenomyosis, had fewer complaint of dysmenorrhea and did not have endometriosis (Table I).

Evidence for increased platelet aggregation, activation of TGF-β/Smad pathway, occurrence of EMT, FMT and SMM, and increased proliferation, MVD and fibrotic content

Platelet aggregation, stained by CD41, was seen mostly in the stromal component of ectopic endometrium and a few control endometrium (Fig. 1), consistent with our findings in endometriosis (Ding *et al.*, 2015). VEGF staining was increased in the cytoplasm of ectopic epithelium as compared with negative staining in control groups (Supplementary Fig. S2). CD31-positive microvessels were found mostly in the stromal tissues, and the MVD was increased significantly in adenomyotic foci as compared with that in the controls. PCNA staining was primarily seen in the nuclei of epithelial cells and some stromal cells in ectopic endometrium, and was significantly increased as compared with the control ones (Figs 1 and 2 and Supplementary Fig. S2).

TGF-β1 was stained positive mostly in the cytoplasm of ectopic endometrial epithelium and also in some stromal cells as compared with negative staining in control endometrium. The staining of p-Smad3—the active form of Smad3—was seen in the nuclei of epithelial cells and some stromal cells in ectopic endometrium, but not in control endometrium. E-cadherin staining was seen almost exclusively in the membrane of epithelial cells of both adenomyotic and control subjects, but its levels were significantly decreased in the former group (Fig. 1). In contrast, vimentin staining was seen mostly in the cytoplasm of stromal cells in control and adenomyosis groups, and also seen in the cytoplasm of epithelial cells in ectopic endometrium. Besides the SMCs, α-SMA staining was also observed in the cytoplasm of both epithelial cells and stromal cells in ectopic endometrium, but not in control endometrium. Collagen I was stained positive in the cytoplasm of epithelial cells and stromal cells in ectopic endometrium, but not in control endometrium. PR-B showed a positive staining in the nuclei of epithelial cells, but was significantly lower in the nuclei of ectopic epithelial cells. LOX was stained positive in the nuclei of epithelial and stromal cells in the ectopic and control endometrium, and the staining level was significantly higher in the former (Supplementary Fig. S2).

We found that the extent of platelet aggregation, MVD, as well as immunoreactivity to VEGF, PCNA, TGF-β1, p-Smad3, vimentin, α-SMA,

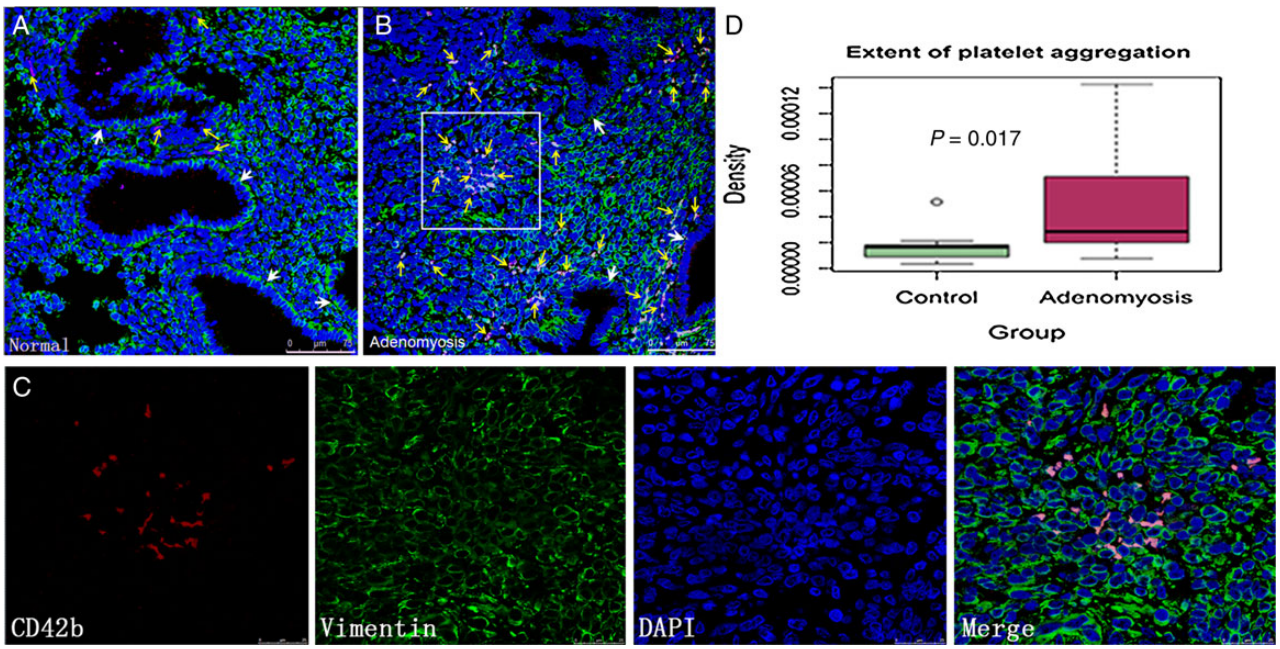

Figure 3 Representative fluorescent photomicrographs of platelet aggregation in adenomyosis and summary results. Immunofluorescent staining of CD42b in normal human endometrium (**A**) and human adenomyotic lesion (**B**), both were in the secretory phase. CD42b and vimentin, stained in red and green, respectively, were used as the marker for platelets and endometrial stromal cells, while DAPI, stained in dark blue, was used as a marker for cell nuclei. The white frame in (B) indicates the area to be magnified and is shown in more detail in (**C**). In both (A) and (B), the yellow arrows indicate the platelet aggregation while the white arrows indicate the glandular epithelium of the lesion (×400). (C) Magnified figure showing aggregated platelets (CD42b-positive, in red), adenomyotic stromal cells (vimentin-positive, in green) and DAPI (cell nuclei, in blue), and co-localization of platelet aggregation and stromal cells (×1000). (**D**) Boxplot of the number of aggregated platelets in control and ectopic endometrium. The number shown in the figure is the *P*-value of the statistical significance of the difference between control and ectopic endometrium.

Downloaded from https://academic.oup.com/humrep/article/31/4/734/2380144 by guest on 21 August 2022

collagen I and LOX were all highly significantly elevated in ectopic endometrium from women with adenomyosis as compared with controls (Fig. 2A–L). In contrast, the immunoreactivity to E-cadherin and PR-B was significantly reduced in ectopic endometrium from women with adenomyosis as compared with controls (Fig. 2A–L). Multiple linear regression analyses using age, menstrual phase, parity, and the source of tissue sample (adenomyosis versus control) indicated that, with the only exception of PR-B in which case the secretory phase was significantly associated with higher PR-B immunoreactivity, the source of tissue sample was the only factor that is associated with these immunoreactivity measures (all P-values <0.01; all $R^2 > 0.58$, except vimentin, in which case $R^2 = 0.24$). That is, after controlling for age, menstrual phase and parity, we still found that the differences in these measurements are highly significant between women with and without adenomyosis.

We also stained for OTR, which is detected only in fully differentiated SMCs (Busnelli *et al.*, 2010), desmin, a marker for differentiated and mature SMC (Hasegawa *et al.*, 2003), and SM-MHC, a marker restricted for the SMC (Manabe and Owens, 2001), in adenomyotic lesions as well as control endometrium. We found that the immunoreactivity to these three markers was significantly higher in adenomyosis than in controls (Fig. 2M–O and Supplementary Fig. S3). Multiple linear regression analyses using age, menstrual phase, parity, and the source of tissue sample (adenomyosis versus control) indicated that the source of tissue sample was the only factor that is associated with these immunoreactivity measures (all P-values <0.001; all $R^2 > 0.87$). Therefore, the immunoreactivity against markers of fully differentiated SMCs in adenomyotic lesions was significantly higher than that of control endometrium.

Further evidence for increased platelet aggregation in adenomyotic lesions

We found that while CD42b-stained platelets were nearly absent in control endometrium (Fig. 3A), they were aggregated mainly in the pericellular spaces of vimentin-positive stromal cells of adenomyotic foci (Fig. 3B). A closer examination of aggregated platelets indicates that they appeared to surround EESCs (Fig. 3C), very similar to that in

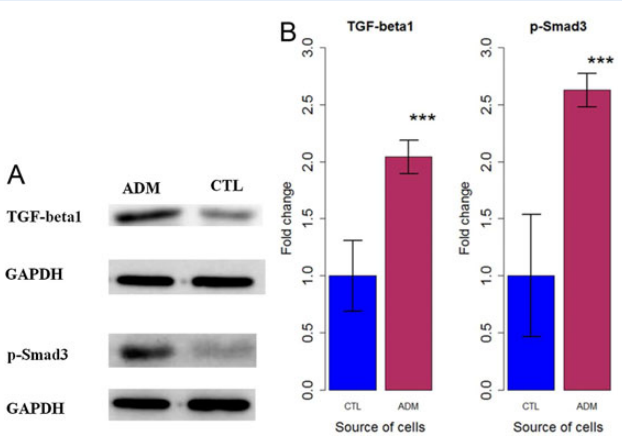

Figure 4 Elevated TGF-β1 and Smad3 protein expression in adenomyosis. (**A**) Representative western blot results for TGF-β1 and p-Smad3. CTL: endometrial stromal cells derived from control endometrium ($n = 8$ subjects); ADM: endometrial stromal cells derived from adenomyotic lesions ($n = 8$ subjects); (**B**) Boxplots of results of TGF-β1 and p-Smad3 protein levels in control and ectopic endometrium. The P-value of between-group difference is shown in the figures.

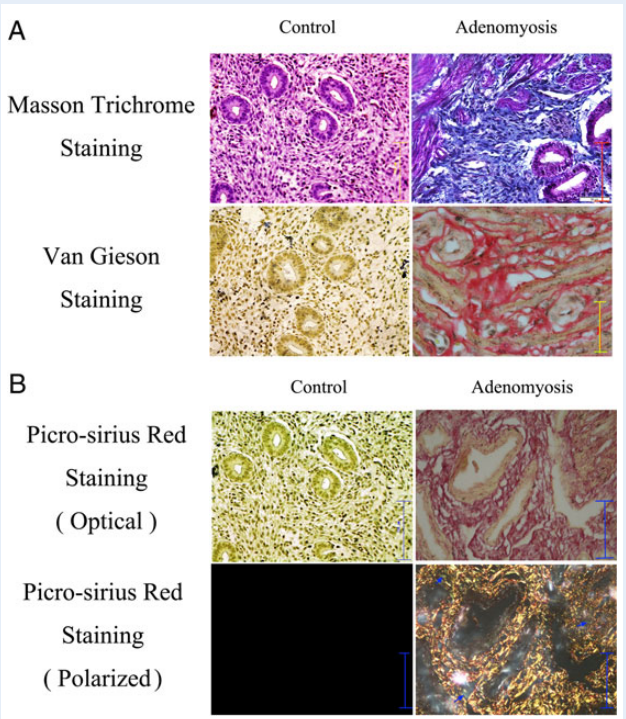

Figure 5 Evidence for increased fibrotic content in adenomyosis. (**A**) Representative photomicrographs of Masson trichrome staining and Van Gieson staining in control and ectopic endometrium. In Masson trichrome staining, collagens are stained in blue, while smooth muscle and epithelial cells are stained in purple. No blue collagen fiber (blue) can be seen in control endometrium, while collagen fibers in the stromal component are prominent in ectopic endometrium from women with adenomyosis. The presence of smooth muscle cells is also visible in ectopic endometrium. In Van Gieson staining, collagens are stained in red, while smooth muscle and epithelial cells are stained in yellow. Consistent with the Masson staining, no collagen fibers (in red) can be seen in control endometrium, but these fibers are conspicuous in the stromal compartment of ectopic endometrium. (**B**) Representative photomicrographs of Picro-sirius red staining visualized under optical (top panel) and polarized microscopy (lower panel). Collagen fibers would appear red while epithelium and muscles would appear yellow under the optical microscopy. Under the polarized microscopy, collagens in the stroma would appear bright (type I, red or yellow and type III, green), respectively, while epithelium, smooth muscles without collagens would appear to be dark/black. In control endometrium, vascular epithelium, myometrium and endometrial epithelium in adenomyotic lesions appeared yellow under the optical microscope, while the ectopic endometrium showed red, suggestive of collagen fibers. No red-stained collagen fiber can be seen in control endometrium but they are very prominent in ectopic endometrium. Similarly, control endometrium and vascular epithelium, myometrium and the epithelial compartment of ectopic endometrium all appeared dark/black. In ectopic endometrium, bright red- or yellow-colored type I collagen fibers and a few green-colored type III collagen fibers (blue arrows) can be seen under the polarized microscope. All scale bars = 125 μm.

Downloaded from https://academic.oup.com/humrep/article/31/4/734/2380144 by guest on 21 August 2022

endometriotic lesions (Ding et al., 2015). After counting the number of CD42b-positive platelets in the ectopic and the control endometrium, we found that the density of platelets in ectopic endometrium is significantly higher in adenomyotic lesions than that in the control endometrium ($P < 0.05$) (Fig. 3D). A multiple linear regression incorporating age, menstrual phase and the source of tissue samples indicates that adenomyotic lesions had a higher density of platelets than control endometrium ($P < 0.05$). This result is consistent with the immunostaining result using different samples.

Evidence for activation of the TGF-β/Smad3 signaling pathway

To confirm the immunohistochemistry finding, we evaluated the protein expression levels of TGF-β1 and p-Smad3 in stromal cells of ectopic and control endometrium. We found that the protein expression levels of TGF-β1 and p-Smad3 were both significantly higher in adenomyotic stromal cells than that of normal endometrial stromal cells (both *P*-values <0.001; Fig. 4A and B).

Evidence for fibrosis in adenomyotic lesions

We also performed Masson trichrome, Van Gieson, and Picro-Sirius red staining of adenomyotic lesions and of control endometrium. All three staining methods indicated that, while in control uteri the staining was all negative for fibrotic tissues, adenomyotic lesions contained quite extensive collagen fibers (Fig. 5). In addition, Masson staining in adenomyotic lesions showed that substantial portions of the stromal compartment were stained red, suggestive of muscle fibers or epithelium cells, with blue fibers indicating collagen fibers (Fig. 5A). The extent of fibrosis correlated positively with the staining levels of desmin, SM-MHC and OTR in the stromal component of adenomyotic lesions (all r's > 0.73, all *P*-values <0.001). Van-Gieson staining showed mostly muscle fibers or epithelium (mostly epithelium), stained yellowish, in control endometrium, while the adenomyotic lesions appeared mostly red indicating collagen fibers (Fig. 5A). Under the optical microscope, the Picro-Sirius red staining in sections of normal endometrium as well as endometrial epithelium and vascular epithelium in adenomyotic lesions appeared yellowish, suggestive of normal epithelial tissues, while the ectopic endometrium showed mostly bright red, indicative of collagen fibers. Under the polarized microscope, the normal endometrium, and the vascular epithelium and the epithelial compartment of ectopic endometrium all appeared dark black, indicating a lack of collagen fibers (Fig. 5B). In contrast, collagen I positive fibers, stained red or yellow, were thick, while collagen III positive fibers, stained in green, were thin in the stromal component of adenomyotic lesions (Fig. 5B).

In addition, the extent of fibrosis, measured by the percentage of fibrotic tissue content via Masson trichrome staining, was significantly higher in adenomyotic lesions than that of control endometrium

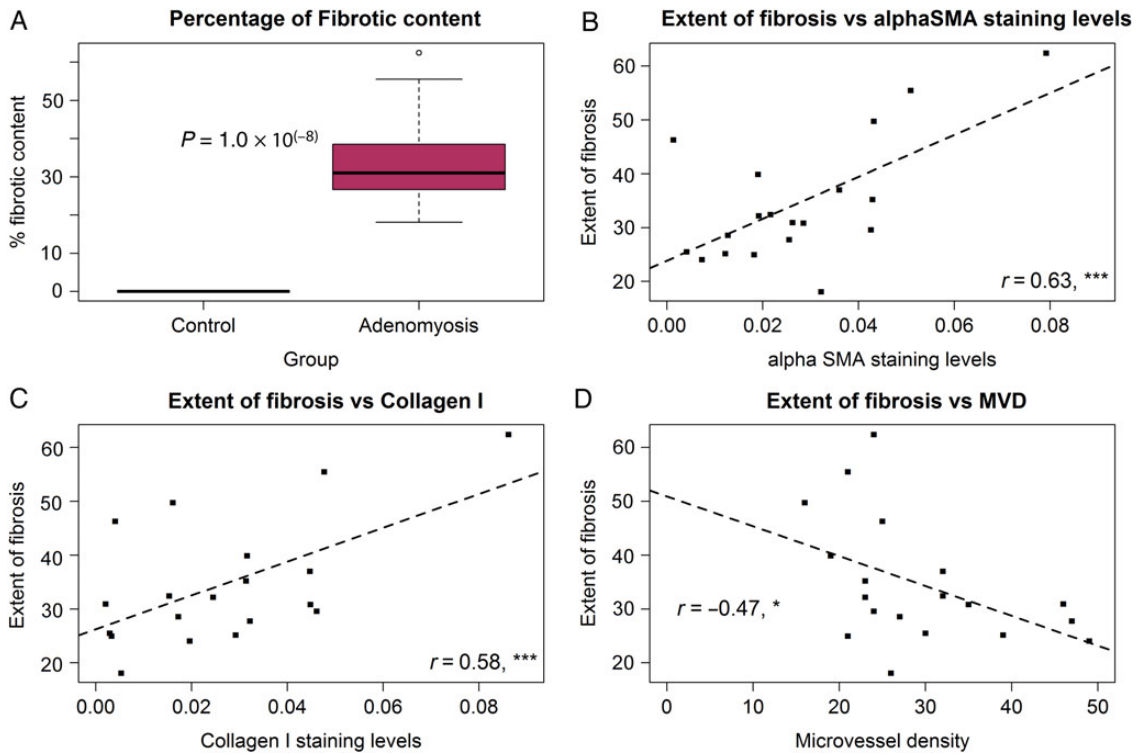

Figure 6 Evidence for smooth muscle metaplasis (SMM), fibrosis and reduced neovasculature in adenomyosis. (**A**) Boxplot showing the percentage of fibrotic content in ectopic and control endometrium as evaluated by Masson trichrome staining. The number shown in the figure is the *P*-value of the statistical significance of the difference. The percentage was taken as 0 for control endometrium since no fibrosis was found. (**B**) Scatter plot of the extent of fibrosis versus the α-SMA staining levels in the ectopic endometrium. (**C**) Scatter plot of the extent of fibrosis versus the collagen I staining levels in the ectopic endometrium. (**D**) Scatter plot of the extent of fibrosis versus the microvessel density (CD31) in the ectopic endometrium. The number in figures (B), (C) and (D) is Pearson's correlation coefficient. *$P < 0.05$; ***$P < 0.001$. The dashed line is the regression line.

Downloaded from https://academic.oup.com/humrep/article/31/4/734/2380144 by guest on 21 August 2022

($P = 1.0 \times 10^{-8}$; Fig. 6A), and the linear regression analyses incorporating age, menstrual phase, parity, and the source of tissue sample indicated that the source of tissue sample was the only factor that is associated with increased extent of fibrosis ($P < 0.001$, $R^2 = 0.95$). Consistently, the extent of fibrosis in adenomyotic lesions correlated positively with the immunoreactivity to α-SMA and collagen I ($r = 0.63$, $P < 0.01$, and $r = 0.58$, $P < 0.01$, respectively; Fig. 6B and C), but not to LOX ($r = 0.07$, $P > 0.05$). Interestingly, the extent of fibrosis in the tissues correlated negatively with the MVD ($r = -0.47$, $P < 0.05$; Fig. 6D). As expected, the α-SMA and collagen I staining levels in adenomyosis were highly correlated ($r = 0.90$, $P < 0.001$).

Other findings

We found that the extent of platelet aggregation in ectopic endometrium correlated positively with the MVD and the immunoreactivity against TGF-β1, VEGF, and PCNA, but not other measures (all square-root transformed to improve normality; Fig. 7). In addition, the uterus size in women with adenomyosis correlated positively with the staining levels of α-SMA, collagen I and the extent of fibrosis, but not with other measures (Fig. 8).

To exploit the possibility that platelets may also be responsible for HGF-mediated EMT in adenomyosis (Khan *et al.*, 2015), we performed immunofluorescent staining of both platelets and HGF in adenomyotic lesions ($n = 10$). We found that platelets and HGF were co-localized mostly in the stromal component of adenomyotic lesions, near the glandular epithelium (Fig. 9), suggesting that platelets may also be responsible for increased HGF content, thereby promoting EMT in adenomyotic lesions.

Discussion

We have presented evidence of increased platelet aggregation in adenomyotic lesions and increased immunostaining and protein levels of TGF-β1 and p-Smad3 in adenomyosis as compared with control endometrium. In addition, we have shown decreased staining of E-cadherin but increased vimentin staining in the epithelial component of adenomyotic lesions that are consistent with EMT as reported in adenomyosis (Chen *et al.*, 2010; Khan *et al.*, 2015). Furthermore, we have shown increased staining of α-SMA, a marker for myofibroblasts, in the stromal component of adenomyotic lesions, suggestive of FMT in adenomyotic lesions. Consistent with this notion, immunoreactivity against collagen I and LOX was significantly increased in adenomyosis, indicating increased ECM production and deposition. More remarkably, we have shown that adenomyotic lesions express desmin, SM-MHC and OTR that are found typically in highly differentiated SMCs. Finally, adenomyotic lesions showed significantly increased fibrotic content, very likely

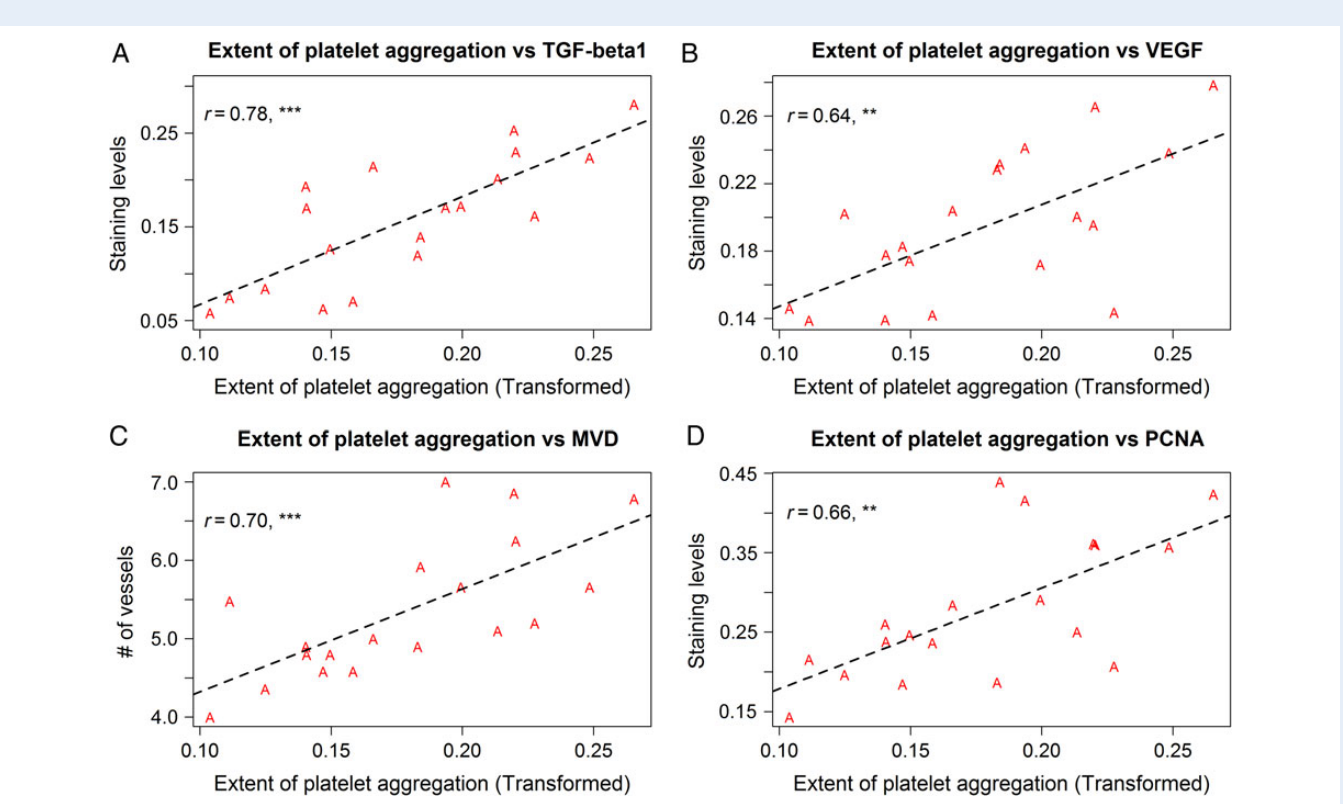

Figure 7 Platelet aggregation and TGF-β1 signaling, angiogenesis and cellular proliferation in adenomyosis. (**A**) Scatter plot showing the extent of platelet aggregation versus the TGF-β1 staining levels in the ectopic endometrium. (**B**) Scatter plot showing the extent of platelet aggregation versus the VEGF staining levels in the ectopic endometrium. (**C**) Scatter plot showing the extent of platelet aggregation versus the microvessel density (CD31) in the ectopic endometrium. (**D**) Scatter plot showing the extent of platelet aggregation versus the PCNA staining levels in the ectopic endometrium. The number in each figure is Pearson's correlation coefficient. $^{**}P < 0.01$; $^{***}P < 0.001$. The dashed line is the regression line. Each dot, labeled by 'A', represents one data point from a patient with adenomyosis.

Downloaded from https://academic.oup.com/humrep/article/31/4/734/2380144 by guest on 21 August 2022

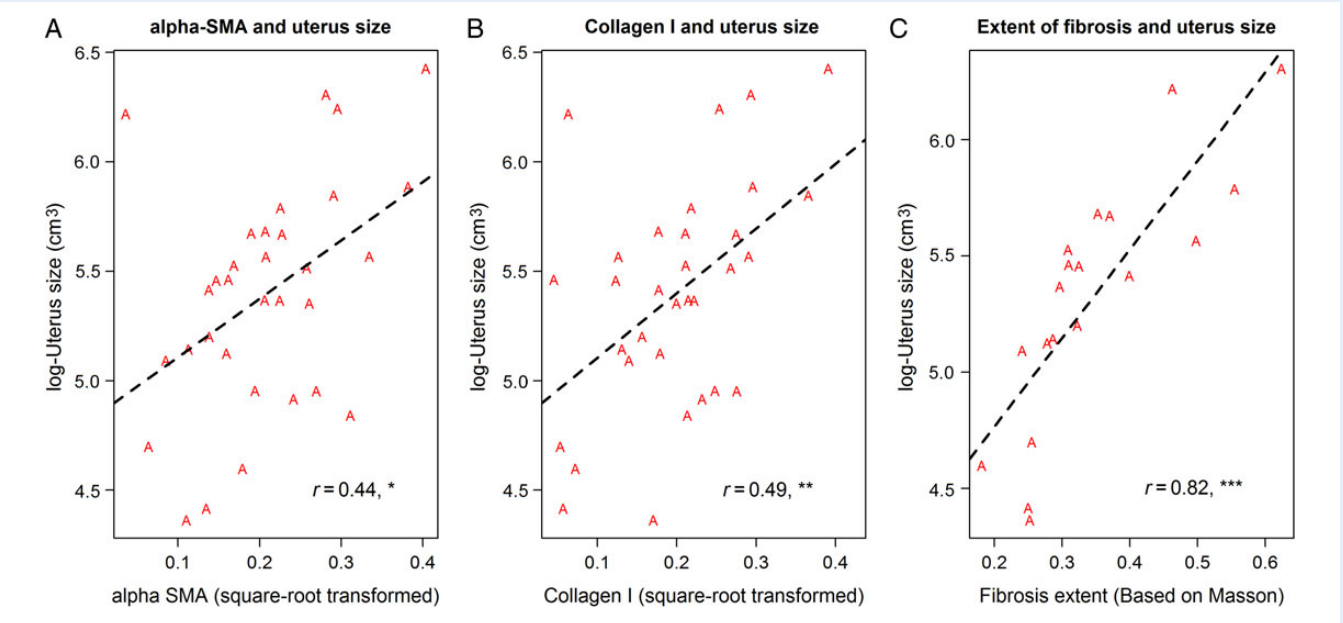

Figure 8 Uterus size and its relationship with the extent of fibrosis and smooth muscle metaplasia. (**A**) Scatter plot showing the relationship between the α-SMA staining levels in the ectopic endometrium and the uterus size in women with adenomyosis; (**B**) Scatter plot showing the relationship between the collagen I staining levels in the ectopic endometrium and the uterus size in women with adenomyosis; (**C**) Scatter plot showing the relationship between the extent of fibrosis in the ectopic endometrium and the uterus size in women with adenomyosis; The number in each figure is Pearson's correlation coefficient. *$P < 0.05$; **$P < 0.01$; ***$P < 0.001$. The dashed line is the regression line. Each dot, labeled by 'A', represents one data point from a patient with adenomyosis.

resulting from EMT and FMT. These results corroborate well with our findings in mouse (Shen *et al.*, 2016) and suggest that adenomyotic lesions are just like endometriotic lesions and undergo platelet-induced activation of the TGF-β/Smad3 signaling pathway, resulting in EMT, FMT and SMM and leading to increased cell contractility, collagen production, and ultimately to fibrosis (Zhang *et al.*, submitted for publication), even though the two conditions may have entirely different etiologies. In addition, adenomyotic lesions appear to have all the necessary molecular machinery to promote fibrogenesis, just like their endometriotic counterpart. Taken together, these data suggest that, despite being two separate disease entities, adenomyosis and endometriosis share the same commonality of being wounds that undergo repeated tissue injury and repair, resulting ultimately in fibrosis (Ding *et al.*, 2015; Guo *et al.*, 2015). This may explain why the two conditions share many similar molecular aberrations.

Our finding of elevated TGF-β1 expression in adenomyosis is in broad agreement with the reported increased TGF-β1 concentration in uterine washings (Inagaki *et al.*, 2003). The decrease in E-cadherin expression and increase in vimentin expression is consistent with reported EMT in adenomyosis (Chen *et al.*, 2010; Khan *et al.*, 2015). The increase in staining of α-SMA, desmin, SM-MHC and OTR in the stromal component of adenomyotic lesions is consistent with the reported presence of SMM in adenomyosis (Mechsner *et al.*, 2010). While fibrosis *per se* has not, to the best of our knowledge, been reported in adenomyosis, the increased collagen content in adenomyosis has been documented, although not in the mainstream journals (Fujita, 1985; Ikegami and Kato, 1992). Interestingly, Robert Meyer described adenomyosis as adenofibromyohyperplasia as early as 1930 in his histologic study of adenomyosis (Meyer, 1930).

Our results may also be consistent with finding by Khan *et al.* (Khan *et al.*, 2015), who showed HGF-mediated EMT in endometrial epithelial cells but did not show where the HGF came from. Following platelet activation, hundreds of biologically active molecules, including HGF (Nakamura *et al.*, 1986; Matsuo *et al.*, 2008), are released and deposited at the sites of a wound (Coppinger *et al.*, 2004) and, as shown in Fig. 9, also in adenomyotic lesions and lesion vasculature. In other words, activated platelets aggregated within the adenomyotic lesions can be the source of HGF that promotes EMT, possibly through paracrine action.

Our finding that uterus size in women with adenomyosis correlated positively with the staining levels of α-SMA, collagen I and the extent of fibrosis seems to suggest that the uterus size is directly proportional to the extent of progression of adenomyosis. This could be due to the fact that when myofibroblasts are stimulated by activated platelets long enough, they acquire markers as well as phenotypes of differentiated SMCs, such as desmin, SM-MHC and OTR (Zhang *et al.*, unpublished data). Since ectopic endometrial stromal cells are in direct contact with the underlying myometrium, which is conducive to cell–cell cross-talk and interaction, these *de novo* SMCs may be fused with myometrial SMCs, resulting in an enlarged uterus.

This scenario is not far-fetched. In fact, one gene expression profiling study reports that after just 36 h of exposure to TGF-β1, human fetal lung fibroblasts expressed caldesmon and SM-MHC (Chambers *et al.*, 2003), markers that are thought to be reserved for differentiated SMC. Similarly, corneal fibroblasts with extended exposure to TGF-β1 and PDGF had increased expression of desmin (Singh *et al.*, 2014), yet activated platelets are known to release PDGF (Coppinger *et al.*, 2004). After all,

Downloaded from https://academic.oup.com/humrep/article/31/4/734/2380144 by guest on 21 August 2022

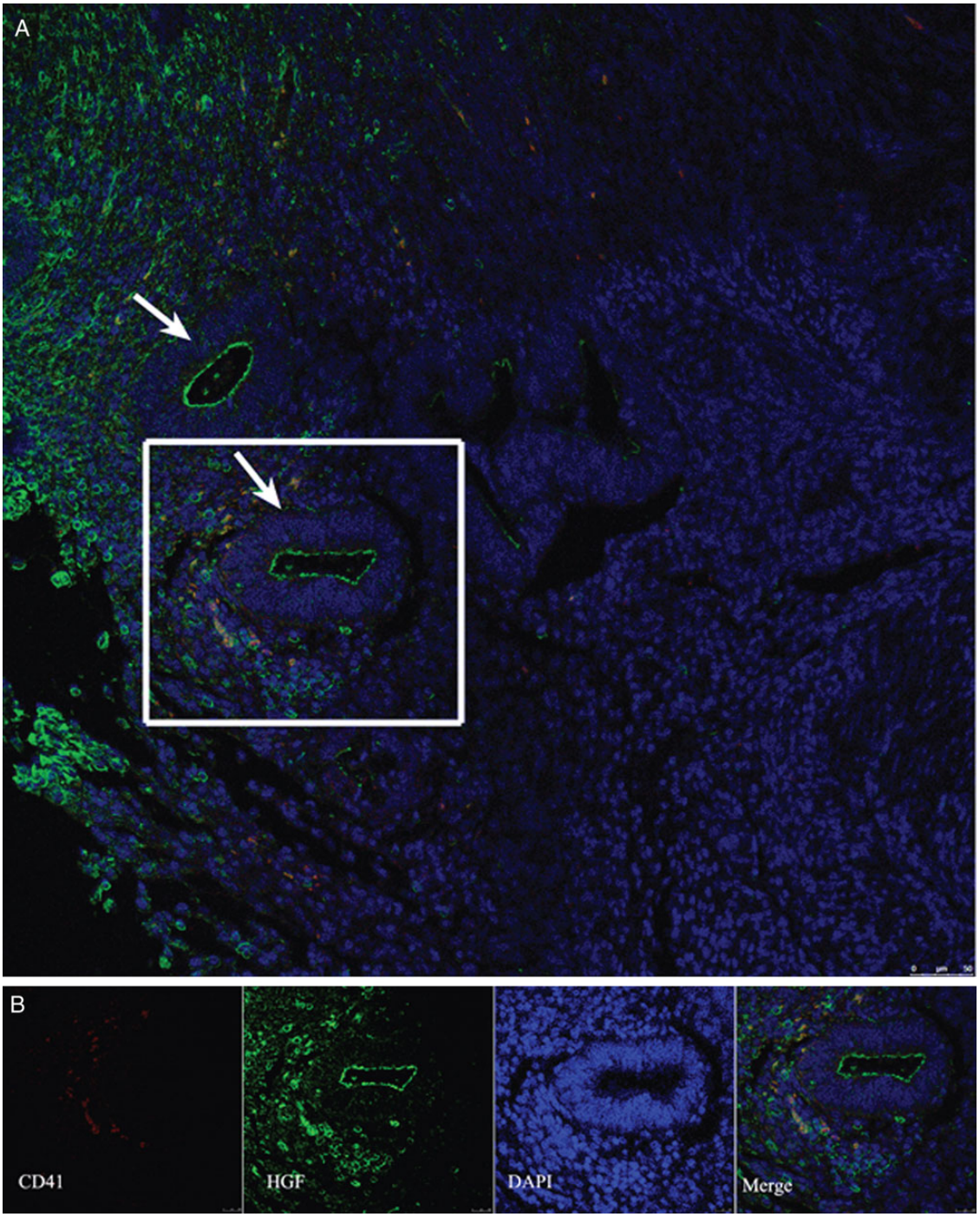

Figure 9 Representative fluorescent photomicrographs of a double staining of HGF and CD41 in adenomyotic lesions. The white frame in (**A**) indicates the area to be magnified and is shown in more detail in (**B**). The arrows in (A) indicate the glandular epithelium of the lesion (×200); (B) Magnified figure showing aggregated platelets (CD41, in red), HGF (in green) and DAPI (cell nuclei, in blue), and co-localization of platelet aggregation and HGF in adenomyotic stromal cells (×400).

physiological transdifferentiation of undifferentiated mesenchymal cells into myometrial SMCs in the junctional zone of the uterus has been previously established (Konishi *et al.*, 1984; Fujii *et al.*, 1989).

Our finding of a negative correlation between the extent of fibrosis and MVD may explain why adenomyosis appears to be resistant to drug treatment. Indeed, increased fibrosis, along with decreased vasculature, would render delivery of any drug to adenomyotic lesions difficult. In addition, decreased PR-B expression, very likely due to PR-B promoter hypermethylation (Jichan *et al.*, 2010), would render adenomyotic lesions non-responsive to hormonal treatment.

Downloaded from https://academic.oup.com/humrep/article/31/4/734/2380144 by guest on 21 August 2022

Adenomyosis has been traditionally viewed as an estrogen-dependent disorder (Kitawaki, 2006), featuring aberrant expression of aromatase and increased production of estrogens (Kitawaki *et al.*, 1997). It is also recognized as an inflammatory disease, as characterized by increased production/expression of proinflammatory cytokines and chemokines (Ulukus *et al.*, 2005, 2006; Benagiano *et al.*, 2014) and the constitutive activation of nuclear factor-κB (Li *et al.*, 2013). A growing body of evidence accumulated in the last two decades suggests that inflammation and coagulation are two major host-defense systems that interact with each other (Lipinski *et al.*, 2011; Petaja, 2011). In fact, the two entities are now known to be intricately interconnected: inflammation activates the coagulation cascade and coagulation modulates the inflammatory activity in many ways (Lipinski *et al.*, 2011; Petaja, 2011), as in cardiovascular disease (Demetz and Ott, 2012). Activated platelets were found to play a critical role in initiating inflammation (Sreeramkumar *et al.*, 2014). In adenomyosis, some platelet adhesion molecules, such as certain integrins, are reported to be aberrantly expressed (Kawahara *et al.*, 2003).

Bleeding is a cardinal sign of vascular injury or tissue injury. But once there is tissue injury, evolutionarily conserved mechanisms in all multicellular organisms dictate that tissue repair becomes of paramount importance. Consequently, each cyclic bleeding experienced by ectopic endometrium in adenomyosis is followed by tissue repair, which is known to involve EMT (Thiery *et al.*, 2009). It also involves myofibroblast activation so that fibroblasts acquire a migratory phenotype in order to re-populate the damaged tissues (Hinz, 2007). However, with repeated and persistent tissue injury and then repair, the normal, physiological wound-healing response can go awry (Wynn, 2007), resulting in excessive ECM deposits, leading to fibrosis (Thannickal *et al.*, 2014). Viewed through this lens, it is easy to understand just how important the platelets are in the development of adenomyosis.

While increased platelet aggregation in adenomyosis has never been reported, we note that our results are nonetheless consistent with our previous report that the expression of tissue factor in adenomyosis is elevated (Liu *et al.*, 2011; Li *et al.*, 2013). Tissue factor plays a critical role in the initiation of platelet activation and coagulation (Engelmann *et al.*, 2003). In addition, considerable experimental data (Mori *et al.*, 1991; Ficicioglu *et al.*, 1995) and limited clinical data (Yu *et al.*, 2015) support the involvement of hyperprolactinemia in adenomyosis, yet prolactin is a potent cofactor for platelet aggregation (Wallaschofski *et al.*, 2001; Urban *et al.*, 2007).

The increased platelet aggregation in adenomyotic lesions, as reported here, may shed new light onto the pathophysiology of adenomyosis. First, following platelet activation, approximately 300 biologically active molecules are released and deposited at sites of a wound (Coppinger *et al.*, 2004), and almost surely within adenomyotic lesions and their surrounding myometrium. In fact, platelets contain many important proteins involved in angiogenesis, proliferation, uterine hyperactivity, and innervation, such as VEGF, thromboxane A2 (TXA_2), brain-derived neurotrophic factor (BDNF), and nerve growth factor (NGF). Platelets are now regarded as the major source of VEGF in serum, as the platelet pool comprises over 80% of total circulating VEGF in patients with cancer as well as healthy individuals (Holmes *et al.*, 2008; Peterson *et al.*, 2010). In some cancers in particular, platelet-derived VEGF better predicts tumor progression than serum levels of VEGF (Jelkmann, 2001). Thus, platelets may well be an important source for the increased angiogenesis seen in adenomyosis (Schindl *et al.*, 2001; Huang *et al.*, 2014). Second, since TXA_2 is known to be an inducer of uterine hyperactivity (Wetzka *et al.*, 1994; Crankshaw, 1995) through TXA_2 receptors, TPs (Moore *et al.*, 2002), which are unaffected by hormones (Senchyna and Crankshaw, 1999), the released TXA_2 by activated platelets may likely promote uterine hyperperistalsis or even dysperistalsis, as documented in adenomyosis (Kunz *et al.*, 1998; Leyendecker *et al.*, 2004; Kissler *et al.*, 2007), since inherently unevenly distributed adenomyotic lesions and thus uneven TXA_2 concentration in the uterus may disrupt synchronized uterine contraction (Kitlas *et al.*, 2009), causing pain. Moreover, platelet-derived NGF and BDNF could be responsible for myometrial hyperinnervation in adenomyosis (Zhang *et al.*, 2010; Barcena de Arellano *et al.*, 2011, 2013).

The important role of platelets in the development of adenomyosis, as unveiled in this and our mouse study (Shen *et al.*, 2016), has practical implications for the development of non-hormonal therapeutics for adenomyosis. While it has recently been shown that epigallocatechin-3-gallate (EGCG) is promising for its anti-fibrotic properties in treating endometriosis (Matsuzaki and Darcha, 2014) and also efficacious in treating adenomyosis in mice with induced adenomyosis (Chen *et al.*, 2013, 2014), it is perhaps no coincidence that EGCG is anti-platelet (Ok *et al.*, 2012). In fact, some compounds that are reported to be promising in treating adenomyosis or endometriosis in preclinical and clinical studies, such as andrographolide (Mao *et al.*, 2011; Li *et al.*, 2013; Liu *et al.*, 2014), valproic acid (Liu and Guo, 2008, 2011; Liu *et al.*, 2010), curcumin (Zhang *et al.*, 2011), resveratrol (Zhu *et al.*, 2015), puerarin (Chen *et al.*, 2011; Wang *et al.*, 2011), and quercetin (Zhang *et al.*, 2009), turn out to be either anti-platelet or antithrombotic (Choo *et al.*, 2002; Liu *et al.*, 2006; Shen *et al.*, 2007; Jin *et al.*, 2008; Mayanglambam *et al.*, 2010; Davidson *et al.*, 2011; Lu *et al.*, 2011; Lien *et al.*, 2013; Mosawy *et al.*, 2013a,b).

In conclusion, we have presented corroborative evidence that is consistent with the notion that platelets play a critical role in driving EMT, FMT and SMM in the development of adenomyosis, leading to increased production of ECM products and ultimately to fibrosis, as we have shown in endometriosis and a mouse model of adenomyosis. These findings, coupled with other possible roles of platelets in the development of adenomyosis as yet to be delineated, shed new light onto the pathophysiology of adenomyosis, underscore the possibility for the use of anti-coagulation therapy in the non-hormonal treatment of adenomyosis, and hold promise for the development of novel biomarkers for adenomyosis.

Supplementary data

Supplementary data are available at http://humrep.oxfordjournals.org/.

Acknowledgements

The authors would like to thank Professor Jin-Sheng Zhang for his expert assistance on the operation of polarized microscope, and also two anonymous reviewers and the Associate Editor for their constructive comments and suggestions made on an earlier version of this manuscript.

Authors' roles

S.-W.G. conceived and designed the study, performed data analysis and data interpretation, and drafted the manuscript. M.H.S. carried out immunohistochemistry analyses and the HGF immunoflurescence study, X.S.L. recruited patients and secured their biological samples,

Downloaded from https://academic.oup.com/humrep/article/31/4/734/2380144 by guest on 21 August 2022

Q.Q. carried out platelet immunoflurescence study, and H.Z. provided expertise in histochemistry analysis. All participated in writing and approved the final version of the manuscript.

Funding

This research was supported in part by grants 81270676 (S.-W.G.), 81471434 (S.-W.G.), 81530040 (S.-W.G.), 81070470 (X.S.L.), and 81370695 (X.S.L.) from the National Science Foundation of China, and grant 2013ZYJB0019 (X.S.L.) from Shanghai Municipal Commission of Health and Family Planning.

Conflict of interest

None declared.

References

Barcena de Arellano ML, Arnold J, Vercellino F, Chiantera V, Schneider A, Mechsner S. Overexpression of nerve growth factor in peritoneal fluid from women with endometriosis may promote neurite outgrowth in endometriotic lesions. *Fertil Steril* 2011;**95**:1123–1126.

Barcena de Arellano ML, Arnold J, Lang H, Vercellino GF, Chiantera V, Schneider A, Mechsner S. Evidence of neurotrophic events due to peritoneal endometriotic lesions. *Cytokine* 2013;**62**:253–261.

Benagiano G, Habiba M, Brosens I. The pathophysiology of uterine adenomyosis: an update. *Fertil Steril* 2012;**98**:572–579.

Benagiano G, Brosens I, Habiba M. Structural and molecular features of the endomyometrium in endometriosis and adenomyosis. *Hum Reprod Update* 2014;**20**:386–402.

Bergeron C, Amant F, Ferenczy A. Pathology and physiopathology of adenomyosis. *Best Pract Res Clin Obstet Gynaecol* 2006;**20**:511–521.

Busnelli M, Rimoldi V, Vigano P, Persani L, Di Blasio AM, Chini B. Oxytocin-induced cell growth proliferation in human myometrial cells and leiomyomas. *Fertil Steril* 2010;**94**:1869–1874.

Chambers RC, Leoni P, Kaminski N, Laurent GJ, Heller RA. Global expression profiling of fibroblast responses to transforming growth factor-beta1 reveals the induction of inhibitor of differentiation-1 and provides evidence of smooth muscle cell phenotypic switching. *Am J Pathol* 2003;**162**:533–546.

Chen YJ, Li HY, Huang CH, Twu NF, Yen MS, Wang PH, Chou TY, Liu YN, Chao KC, Yang MH. Oestrogen-induced epithelial-mesenchymal transition of endometrial epithelial cells contributes to the development of adenomyosis. *J Pathol* 2010;**222**:261–270.

Chen Y, Chen C, Shi S, Han J, Wang J, Hu J, Liu Y, Cai Z, Yu C. Endometriotic implants regress in rat models treated with puerarin by decreasing estradiol level. *Reprod Sci* 2011;**18**:886–891.

Chen Y, Zhu B, Zhang H, Liu X, Guo SW. Epigallocatechin-3-gallate reduces myometrial infiltration, uterine hyperactivity, and stress levels and alleviates generalized hyperalgesia in mice induced with adenomyosis. *Reprod Sci* 2013;**20**:1478–1491.

Chen Y, Zhu B, Zhang H, Ding D, Liu X, Guo SW. Possible loss of GABAergic inhibition in mice with induced adenomyosis and treatment with epigallocatechin-3-gallate attenuates the loss with improved hyperalgesia. *Reprod Sci* 2014;**21**:869–882.

Choo MK, Park EK, Yoon HK, Kim DH. Antithrombotic and antiallergic activities of daidzein, a metabolite of puerarin and daidzin produced by human intestinal microflora. *Biol Pharm Bull* 2002;**25**:1328–1332.

Coppinger JA, Cagney G, Toomey S, Kislinger T, Belton O, McRedmond JP, Cahill DJ, Emili A, Fitzgerald DJ, Maguire PB. Characterization of the proteins released from activated platelets leads to localization of novel platelet proteins in human atherosclerotic lesions. *Blood* 2004;**103**:2096–2104.

Crankshaw D. Effects of the isoprostane, 8-epi-prostaglandin F2 alpha, on the contractility of the human myometrium in vitro. *Eur J Pharmacol* 1995; **285**:151–158.

Davidson DC, Hirschman MP, Spinelli SL, Morrell CN, Schifitto G, Phipps RP, Maggirwar SB. Antiplatelet activity of valproic acid contributes to decreased soluble CD40 ligand production in HIV type 1-infected individuals. *J Immunol* 2011;**186**:584–591.

Demetz G, Ott I. The interface between inflammation and coagulation in cardiovascular disease. *Int J Inflam* 2012;**2012**:860301.

Ding D, Liu X, Duan J, Guo SW. Platelets are an unindicted culprit in the development of endometriosis: clinical and experimental evidence. *Hum Reprod* 2015;**30**:812–832.

Engelmann B, Luther T, Muller I. Intravascular tissue factor pathway—a model for rapid initiation of coagulation within the blood vessel. *Thromb Haemost* 2003;**89**:3–8.

Farquhar C, Brosens I. Medical and surgical management of adenomyosis. *Best Pract Res Clin Obstet Gynaecol* 2006;**20**:603–616.

Ficicioglu C, Tekin HI, Arioglu PF, Okar I. A murine model of adenomyosis: the effects of hyperprolactinemia induced by fluoxetine hydrochloride, a selective serotonin reuptake inhibitor, on adenomyosis induction in Wistar albino rats. *Acta Eur Fertil* 1995;**26**:75–79.

Fujii S, Konishi I, Mori T. Smooth muscle differentiation at endometrio-myometrial junction. An ultrastructural study. *Virchows Arch A Pathol Anat Histopathol* 1989;**414**:105–112.

Fujita M. [Histological and biochemical studies of collagen in human uterine leiomyomas]. *Hokkaido Igaku Zasshi* 1985;**60**:602–615.

Grow DR, Filer RB. Treatment of adenomyosis with long-term GnRH analogues: a case report. *Obstet Gynecol* 1991;**78**:538–539.

Guo SW, Ding D, Shen M, Liu X. Dating endometriotic ovarian cysts based on the content of cyst fluid and its potential clinical implications. *Reprod Sci* 2015;**22**:873–883.

Hasegawa T, Hasegawa F, Hirose T, Sano T, Matsuno Y. Expression of smooth muscle markers in so called malignant fibrous histiocytomas. *J Clin Pathol* 2003;**56**:666–671.

Hernandez Guerrero CA, Bujalil Montenegro L, de la Jara Diaz J, Mier Cabrera J, Bouchan Valencia P. Endometriosis and deficient intake of antioxidants molecules related to peripheral and peritoneal oxidative stress. *Ginecol Obstet Mex* 2006;**74**:20–28.

Hinz B. Formation and function of the myofibroblast during tissue repair. *J Invest Dermatol* 2007;**127**:526–537.

Holmes CE, Huang JC, Pace TR, Howard AB, Muss HB. Tamoxifen and aromatase inhibitors differentially affect vascular endothelial growth factor and endostatin levels in women with breast cancer. *Clin Cancer Res* 2008;**14**:3070–3076.

Huang TS, Chen YJ, Chou TY, Chen CY, Li HY, Huang BS, Tsai HW, Lan HY, Chang CH, Twu NF *et al.* Oestrogen-induced angiogenesis promotes adenomyosis by activating the Slug-VEGF axis in endometrial epithelial cells. *J Cell Mol Med* 2014;**18**:1358–1371.

Ikegami A, Kato J. [Immunohistochemical study of collagen type III in adenomyosis]. *Nippon Sanka Fujinka Gakkai Zasshi* 1992;**44**: 336–340.

Inagaki N, Ung L, Otani T, Wilkinson D, Lopata A. Uterine cavity matrix metalloproteinases and cytokines in patients with leiomyoma, adenomyosis or endometrial polyp. *Eur J Obstet Gynecol Reprod Biol* 2003;**111**:197–203.

Inhaka R, Gentleman RR. R: a language for data analysis and graphics. *J Comput Graph Stat* 1996;**5**:1923–1927.

Itoga T, Matsumoto T, Takeuchi H, Yamasaki S, Sasahara N, Hoshi T, Kinoshita K. Fibrosis and smooth muscle metaplasia in rectovaginal endometriosis. *Pathol Int* 2003;**53**:371–375.

Downloaded from https://academic.oup.com/humrep/article/31/4/734/2380144 by guest on 21 August 2022

Jelkmann W. Pitfalls in the measurement of circulating vascular endothelial growth factor. *Clin Chem* 2001;**47**:617–623.

Jichan N, Xishi L, Guo SW. Promoter hypermethylation of progesterone receptor isoform B (PR-B) in adenomyosis and its rectification by a histone deacetylase inhibitor and a demethylation agent. *Reprod Sci* 2010;**17**:995–1005.

Jin YR, Im JH, Park ES, Cho MR, Han XH, Lee JJ, Lim Y, Kim TJ, Yun YP. Antiplatelet activity of epigallocatechin gallate is mediated by the inhibition of PLCgamma2 phosphorylation, elevation of PGD2 production, and maintaining calcium-ATPase activity. *J Cardiovasc Pharmacol* 2008;**51**:45–54.

Kawahara R, Matsuda M, Mori T. Increase in the number of integrinbeta1-immunoreactive monocyte-lineage cells in experimentally-induced adenomyosis in mice. *Life Sci* 2003;**73**:907–916.

Khan KN, Kitajima M, Hiraki K, Fujishita A, Nakashima M, Masuzaki H. Involvement of hepatocyte growth factor-induced epithelial-mesenchymal transition in human adenomyosis. *Biol Reprod* 2015;**92**:1–11.

Kissler S, Zangos S, Wiegratz I, Kohl J, Rody A, Gaetje R, Doebert N, Wildt L, Kunz G, Leyendecker G *et al.* Utero-tubal sperm transport and its impairment in endometriosis and adenomyosis. *Ann N Y Acad Sci* 2007; **1101**:38–48.

Kitawaki J. Adenomyosis: the pathophysiology of an oestrogen-dependent disease. *Best Pract Res Clin Obstet Gynaecol* 2006;**20**:493–502.

Kitawaki J, Noguchi T, Amatsu T, Maeda K, Tsukamoto K, Yamamoto T, Fushiki S, Osawa Y, Honjo H. Expression of aromatase cytochrome P450 protein and messenger ribonucleic acid in human endometriotic and adenomyotic tissues but not in normal endometrium. *Biol Reprod* 1997;**57**:514–519.

Kitlas A, Oczeretko E, Swiatecka J, Borowska M, Laudanski T. Uterine contraction signals—application of the linear synchronization measures. *Eur J Obstet Gynecol Reprod Biol* 2009;**144**(Suppl 1):S61–S64.

Konishi I, Fujii S, Okamura H, Mori T. Development of smooth muscle in the human fetal uterus: an ultrastructural study. *J Anat* 1984;**139**(Pt 2):239–252.

Kunz G, Noe M, Herbertz M, Leyendecker G. Uterine peristalsis during the follicular phase of the menstrual cycle: effects of oestrogen, antioestrogen and oxytocin. *Hum Reprod Update* 1998;**4**:647–654.

Leyendecker G, Kunz G, Herbertz M, Beil D, Huppert P, Mall G, Kissler S, Noe M, Wildt L. Uterine peristaltic activity and the development of endometriosis. *Ann N Y Acad Sci* 2004;**1034**:338–355.

Li B, Chen M, Liu X, Guo SW. Constitutive and tumor necrosis factor-alpha-induced activation of nuclear factor-kappaB in adenomyosis and its inhibition by andrographolide. *Fertil Steril* 2013;**100**:568–577.

Lien LM, Su CC, Hsu WH, Lu WJ, Chung CL, Yen TL, Chiu HC, Sheu JR, Lin KH. Mechanisms of andrographolide-induced platelet apoptosis in human platelets: regulatory roles of the extrinsic apoptotic pathway. *Phytother Res* 2013;**27**:1671–1677.

Lipinski S, Bremer L, Lammers T, Thieme F, Schreiber S, Rosenstiel P. Coagulation and inflammation. Molecular insights and diagnostic implications. *Hamostaseologie* 2011;**31**:94–102, 104.

Liu X, Guo SW. A pilot study on the off-label use of valproic acid to treat adenomyosis. *Fertil Steril* 2008;**89**:246–250.

Liu X, Guo SW. Valproic acid alleviates generalized hyperalgesia in mice with induced adenomyosis. *J Obstet Gynaecol Res* 2011;**37**:696–708.

Liu R, Xing D, Lu H, Wu H, Du L. Pharmacokinetics of puerarin and ginsenoside Rg1 of CBN injection and the relation with platelet aggregation in rats. *Am J Chin Med* 2006;**34**:1037–1045.

Liu X, Lei Y, Guo SW. Valproic acid as a therapy for adenomyosis: a comparative case series. *Reprod Sci* 2010;**17**:904–912.

Liu X, Nie J, Guo SW. Elevated immunoreactivity to tissue factor and its association with dysmenorrhea severity and the amount of menses in adenomyosis. *Hum Reprod* 2011;**26**:337–345.

Liu X, Yu S, Guo SW. A pilot study on the use of andrographolide to treat symptomatic adenomyosis. *Gynecol Minim Invas Ther* 2014;**3**:119–126.

Lu WJ, Lee JJ, Chou DS, Jayakumar T, Fong TH, Hsiao G, Sheu JR. A novel role of andrographolide, an NF-kappa B inhibitor, on inhibition of platelet activation: the pivotal mechanisms of endothelial nitric oxide synthase/cyclic GMP. *J Mol Med (Berl)* 2011;**89**:1261–1273.

Manabe I, Owens GK. The smooth muscle myosin heavy chain gene exhibits smooth muscle subtype-selective modular regulation in vivo. *J Biol Chem* 2001;**276**:39076–39087.

Mao X, Wang Y, Carter AV, Zhen X, Guo SW. The retardation of myometrial infiltration, reduction of uterine contractility, and alleviation of generalized hyperalgesia in mice with induced adenomyosis by levo-tetrahydropalmatine (l-THP) and andrographolide. *Reprod Sci* 2011;**18**:1025–1037.

Matsuo R, Ohkohchi N, Murata S, Ikeda O, Nakano Y, Watanabe M, Hisakura K, Myronovych A, Kubota T, Narimatsu H *et al.* Platelets strongly induce hepatocyte proliferation with IGF-1 and HGF in vitro. *J Surg Res* 2008;**145**:279–286.

Matsuzaki S, Darcha C. Involvement of the Wnt/beta-catenin signaling pathway in the cellular and molecular mechanisms of fibrosis in endometriosis. *PLoS One* 2013;**8**:e76808.

Matsuzaki S, Darcha C. Antifibrotic properties of epigallocatechin-3-gallate in endometriosis. *Hum Reprod* 2014;**29**:1677–1687.

Mayanglambam A, Dangelmaier CA, Thomas D, Damodar Reddy C, Daniel JL, Kunapuli SP. Curcumin inhibits GPVI-mediated platelet activation by interfering with the kinase activity of Syk and the subsequent activation of PLCgamma2. *Platelets* 2010;**21**:211–220.

Mechsner S, Grum B, Gericke C, Loddenkemper C, Dudenhausen JW, Ebert AD. Possible roles of oxytocin receptor and vasopressin-1alpha receptor in the pathomechanism of dysperistalsis and dysmenorrhea in patients with adenomyosis uteri. *Fertil Steril* 2010;**94**:2541–2546.

Meyer R. Adenofibrosis und adenomyosis. In: (Hrsg.) Stoeckel W (ed) *Johann Veit's Handbuch der Gynakologie*. Berlin: J. F. Bergmann, 1930, 511–515.

Moore F, Asboth G, Lopez BA. Thromboxane receptor signalling in human myometrial cells. *Prostaglandins Other Lipid Mediat* 2002;**67**:31–47.

Mori T, Singtripop T, Kawashima S. Animal model of uterine adenomyosis: is prolactin a potent inducer of adenomyosis in mice? *Am J Obstet Gynecol* 1991;**165**:232–234.

Mosawy S, Jackson DE, Woodman OL, Linden MD. Inhibition of platelet-mediated arterial thrombosis and platelet granule exocytosis by 3′,4′-dihydroxyflavonol and quercetin. *Platelets* 2013a;**24**:594–604.

Mosawy S, Jackson DE, Woodman OL, Linden MD. Treatment with quercetin and 3′,4′-dihydroxyflavonol inhibits platelet function and reduces thrombus formation in vivo. *J Thromb Thrombolysis* 2013b; **36**:50–57.

Nakamura T, Teramoto H, Ichihara A. Purification and characterization of a growth factor from rat platelets for mature parenchymal hepatocytes in primary cultures. *Proc Natl Acad Sci USA* 1986;**83**:6489–6493.

Nawshad A, LaGamba D, Hay ED. Transforming growth factor beta (TGFbeta) signalling in palatal growth, apoptosis and epithelial mesenchymal transformation (EMT). *Arch Oral Biol* 2004;**49**:675–689.

Oh SJ, Shin JH, Kim TH, Lee HS, Yoo JY, Ahn JY, Broaddus RR, Taketo MM, Lydon JP, Leach RE *et al.* beta-Catenin activation contributes to the pathogenesis of adenomyosis through epithelial-mesenchymal transition. *J Pathol* 2013;**231**:210–222.

Ok WJ, Cho HJ, Kim HH, Lee DH, Kang HY, Kwon HW, Rhee MH, Kim M, Park HJ. Epigallocatechin-3-gallate has an anti-platelet effect in a cyclic AMP-dependent manner. *J Atheroscler Thromb* 2012;**19**:337–348.

Parrott E, Butterworth M, Green A, White IN, Greaves P. Adenomyosis—a result of disordered stromal differentiation. *Am J Pathol* 2001;**159**:623–630.

Petaja J. Inflammation and coagulation. An overview. *Thromb Res* 2011; **127**(Suppl 2):S34–S37.

Peterson JE, Zurakowski D, Italiano JE Jr, Michel LV, Fox L, Klement GL, Folkman J. Normal ranges of angiogenesis regulatory proteins in human platelets. *Am J Hematol* 2010;**85**:487–493.

Downloaded from https://academic.oup.com/humrep/article/31/4/734/2380144 by guest on 21 August 2022

Ryan IP, Schriock ED, Taylor RN. Isolation, characterization, and comparison of human endometrial and endometriosis cells in vitro. *J Clin Endocrinol Metab* 1994;**78**:642–649.

Schindl M, Birner P, Obermair A, Kiesel L, Wenzl R. Increased microvessel density in adenomyosis uteri. *Fertil Steril* 2001;**75**:131–135.

Senchyna M, Crankshaw DJ. Operational correlates of prostanoid TP receptor expression in human non-pregnant myometrium are unaffected by excision site or menstrual cycle status of the donor. *Br J Pharmacol* 1999;**128**:1524–1528.

Shen MY, Hsiao G, Liu CL, Fong TH, Lin KH, Chou DS, Sheu JR. Inhibitory mechanisms of resveratrol in platelet activation: pivotal roles of p38 MAPK and NO/cyclic GMP. *Br J Haematol* 2007;**139**:475–485.

Shen F, Liu X, Geng JG, Guo SW. Increased immunoreactivity to SLIT/ROBO1 in ovarian endometriomas: a likely constituent biomarker for recurrence. *Am J Pathol* 2009;**175**:479–488.

Shen M, Liu X, Zhang H, Guo SW. Transforming growth factor β1 signaling coincides with epithelial-mesenchymal transition and fibroblast-to-myofibroblast transdifferentiation in the development of adenomyosis in mice. *Hum Reprod* 2016;**31**:355–369.

Singh V, Barbosa FL, Torricelli AA, Santhiago MR, Wilson SE. Transforming growth factor beta and platelet-derived growth factor modulation of myofibroblast development from corneal fibroblasts in vitro. *Exp Eye Res* 2014;**120**:152–160.

Sreeramkumar V, Adrover JM, Ballesteros I, Cuartero MI, Rossaint J, Bilbao I, Nacher M, Pitaval C, Radovanovic I, Fukui Y *et al.* Neutrophils scan for activated platelets to initiate inflammation. *Science* 2014;**346**:1234–1238.

Thannickal VJ, Zhou Y, Gaggar A, Duncan SR. Fibrosis: ultimate and proximate causes. *J Clin Invest* 2014;**124**:4673–4677.

Thiery JP, Acloque H, Huang RY, Nieto MA. Epithelial-mesenchymal transitions in development and disease. *Cell* 2009;**139**:871–890.

Tukey JW. *Exploratory Data Analysis*. Reading, MA: Addison-Wesley, 1977.

Ulukus EC, Ulukus M, Seval Y, Zheng W, Arici A. Expression of interleukin-8 and monocyte chemotactic protein-1 in adenomyosis. *Hum Reprod* 2005;**20**:2958–2963.

Ulukus M, Ulukus EC, Seval Y, Cinar O, Zheng W, Arici A. Expression of interleukin-8 receptors in patients with adenomyosis. *Fertil Steril* 2006;**85**:714–720.

Urban A, Masopust J, Maly R, Hosak L, Kalnicka D. Prolactin as a factor for increased platelet aggregation. *Neuro Endocrinol Lett* 2007;**28**:518–523.

Wallaschofski H, Donne M, Eigenthaler M, Hentschel B, Faber R, Stepan H, Koksch M, Lohmann T. PRL as a novel potent cofactor for platelet aggregation. *J Clin Endocrinol Metab* 2001;**86**:5912–5919.

Wang D, Liu Y, Han J, Zai D, Ji M, Cheng W, Xu L, Yang L, He M, Ni J *et al.* Puerarin suppresses invasion and vascularization of endometriosis tissue stimulated by 17beta-estradiol. *PLoS One* 2011;**6**:e25011.

Wetzka B, Schafer W, Kommoss F, Bettendorf H, Nusing R, Breckwoldt M, Zahradnik HP. Immunohistochemical localization of thromboxane synthase in human intrauterine tissues. *Placenta* 1994;**15**:389–398.

Wynn TA. Common and unique mechanisms regulate fibrosis in various fibroproliferative diseases. *J Clin Invest* 2007;**117**:524–529.

Yu Y, Jing Z, Zhi-Yu H, Xia M, Yan-Li H, Chang-Tao X, Rui-Fang X, Bing-Song Z. Ultrasound-guided percutaneous microwave ablation for adenomyosis: efficacy of treatment and effect on ovarian function. *Sci Rep* 2015;**5**:10034.

Zhang X, Wang X, Wang HJ, Yang Q, Qie MR. Inhibition effect and mechanisms of quercetin on surgically induced endometriosis. *Sichuan Da Xue Xue Bao Yi Xue Ban* 2009;**40**:228–231, 244.

Zhang X, Lu B, Huang X, Xu H, Zhou C, Lin J. Innervation of endometrium and myometrium in women with painful adenomyosis and uterine fibroids. *Fertil Steril* 2010;**94**:730–737.

Zhang Y, Cao H, Hu YY, Wang H, Zhang CJ. Inhibitory effect of curcumin on angiogenesis in ectopic endometrium of rats with experimental endometriosis. *Int J Mol Med* 2011;**27**:87–94.

Zhu B, Chen Y, Zhang H, Liu X, Guo SW. Resveratrol reduces myometrial infiltration, uterine hyperactivity, and stress levels and alleviates generalized hyperalgesia in mice with induced adenomyosis. *Reprod Sci* 2015;**22**:1336–1349.

Downloaded from https://academic.oup.com/humrep/article/31/4/734/2380144 by guest on 21 August 2022